OPEN ACCESS

Environment & Ecology ARTICLE

Unequal futures: Projecting lake trophic states in China under landscape transformation scenarios

Xinying Shi,[1] Dehua Mao,[1,*] Ling Luo,[1] Kaishan Song,[1] Hongtao Duan,[2] Sijia Li,[1] Chong Fang,[1] Dong Liu,[2] Hui Tao,[1] Hengxing Xiang,[1] and Zongming Wang[1,3]

*Correspondence: maodehua@iga.ac.cn

Received: January 12, 2026; Accepted: July 10, 2026; Published Online: July 21, 2026; https://doi.org/10.59717/j.xinn-geo.2026.100247

GRAPHICAL ABSTRACT

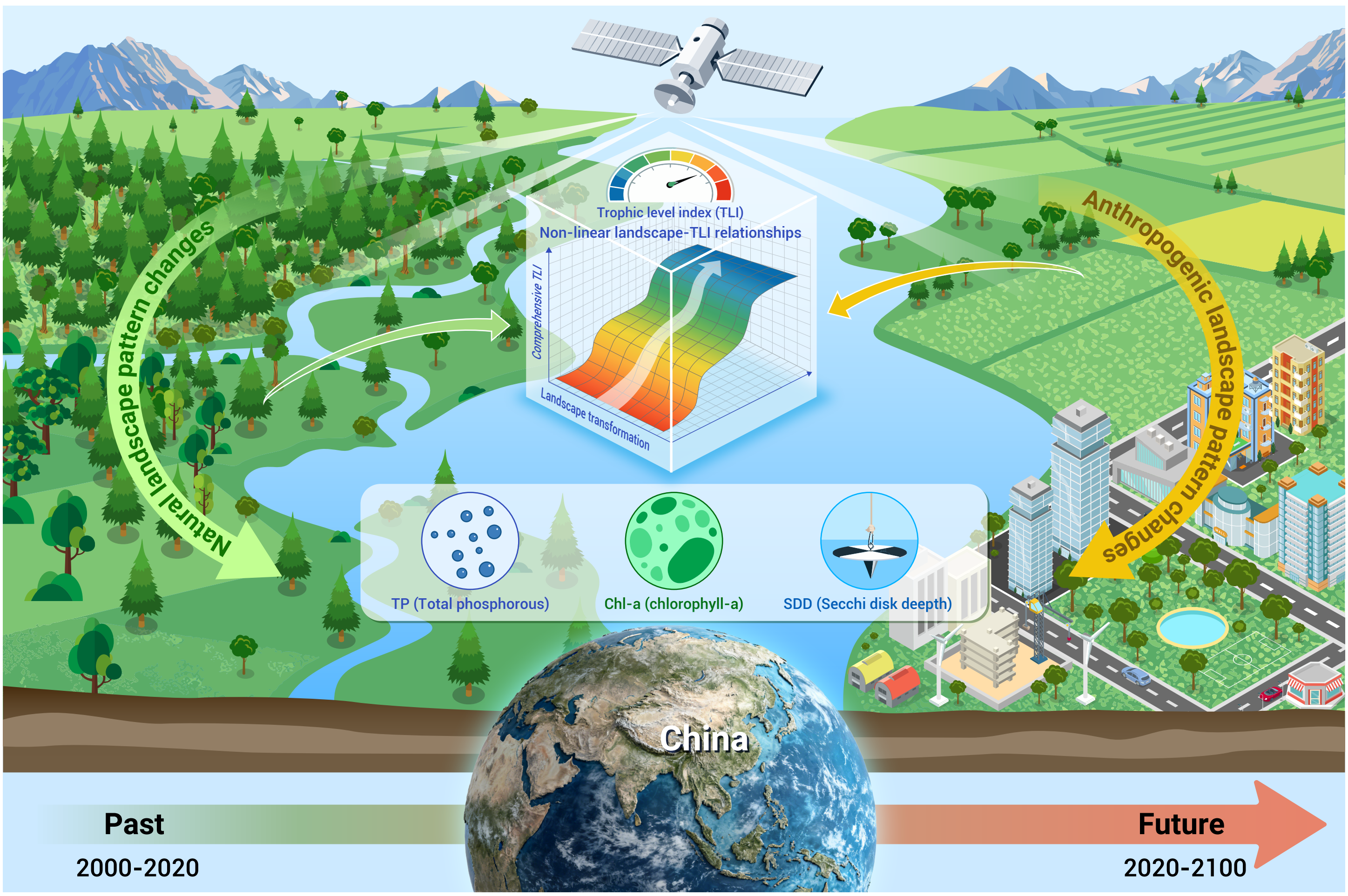

PUBLIC SUMMARY

- Lakes on Yunnan-Guizhou Plateau are most sensitive to landscape changes.
- Model explanations guide threshold-based planning to prevent eutrophication across regions.
- Future biofuel cropland growth along scenario RCP2.6 should avoid sacrificing water quality.

ARTICLE Environment & Ecology

Unequal futures: Projecting lake trophic states in China under landscape transformation scenarios

Xinying Shi,[1] Dehua Mao,[1,*] Ling Luo,[1] Kaishan Song,[1] Hongtao Duan,[2] Sijia Li,[1] Chong Fang,[1] Dong Liu,[2] Hui Tao,[1] Hengxing Xiang,[1] and Zongming Wang[1,3]

[1]Key Laboratory of Black Soils Conservation and Utilization, Northeast Institute of Geography and Agroecology, Chinese Academy of Sciences, Changchun 130102, China

[2]Key Laboratory of Lake Science and Environment, Nanjing Institute of Geography and Limnology, Chinese Academy of Sciences, Nanjing 210008, China

[3]National Earth System Science Data Center, Beijing 100101, China

*Correspondence: maodehua@iga.ac.cn

Received: January 12, 2026; Accepted: July 10, 2026; Published Online: July 21, 2026; https://doi.org/10.59717/j.xinn-geo.2026.100247

Citation: Shi X., Mao D., Luo L., et al. (2026). Unequal futures: Projecting lake trophic states in China under landscape transformation scenarios. *The Innovation Geoscience* 4:100247.

Landscape transformations driven by China's rapid development have contributed to widespread lake eutrophication, but their spatial heterogeneity, underlying mechanisms, and future trajectories remain unclear. We assessed the comprehensive trophic level index (TLI) for 443 Chinese lakes from 2000 to 2020 using integrated datasets of chlorophyll-a (Chl-a), total phosphorus (TP), and Secchi disk depth (SDD) datasets. We modeled TLI responses to landscape changes using an interpretable machine-learning framework. Our findings revealed a national decline in eutrophic lakes (TLI > 50) from 69.1% to 44.2% by 2020, but trends varied regionally. Northwestern lakes improved significantly, with remarkable increases in SDD associated with a 1.2%–2.4% reduction in barren land, whereas southeastern lakes faced persistent pressures from impervious land expansion, with TP rising 6%–10%. Landscape dynamics accounted for 43.9% (Eastern Plain) to 70.1% (Yunnan-Guizhou Plateau) variations in TLI. In the northwest, natural landscape configuration (e.g., woodland largest-patch index) was the strongest predictor. In the southeast, anthropogenic landscape complexity dominated lake trophic dynamics. Land-use projections under Representative Concentration Pathway (RCP) 2.6 indicate potential TLI increases in the Yunnan-Guizhou Plateau, Xinjiang, and Tibetan Plateau due to cropland expansion. RCP8.5 projections produce greater spatial inequality in TLI by 2100. Our findings underscore the necessity for region-tailored land-use strategies to ensure equitable water-quality outcomes under future landscape transformations and to optimize water–food–energy nexus.

INTRODUCTION

Eutrophication of lakes, which hold nearly 90% of surface freshwater,[1] is a growing global concern due to its impacts on ecosystems and human health.[2-4] Anthropogenic and climate-driven basin landscape transformations affect lake trophic states by altering the hydrological and biogeochemical processes of nutrient generation, transport, and transformation.[5,6] Given their lack of strong throughflow for self-purification, lakes are highly sensitive to local landscape changes and to consequent shifts in nutrient dynamics.[7,8] Runoff through expanding agricultural and urban areas is the primary source of excess nitrogen and phosphorus in lakes,[3,9] leading to eutrophication and its consequences, such as deoxygenation, harmful algal blooms, public health risks, increased carbon emissions, and economic losses.[10-13] Clarifying how basin landscape transformations influence lake trophic states is therefore essential for protecting limnetic ecosystems.

Landscape transformations involve changes in both the composition (proportion of land cover classes) and the spatial configuration (e.g., connectivity and fragmentation),[14] directly altering nutrient delivery to lakes through surface runoff and subsurface drainage while indirectly influencing trophic dynamics by altering evaporative demands, hydrological regimes, and biogeochemical cycles.[5,15] Landscape composition impacts nutrient generation and its initial quantities entering the aquatic environment,[16] while configuration governs the transport, interception, transformation, and purification processes before nutrients enter lakes.[5] Notably, landscape pattern changes can produce nonlinear and sometimes opposite outcomes. For example, large contiguous impervious patches (high Largest Patch Index, LPI) were generally believed to exacerbate nutrient loads in urban runoff,[17-19] while dispersed urban sprawl may fragment natural habitats and induce eutrophication in other ways.[20] Such conflicting findings highlight the need for comprehensive analyses that can resolve nonlinear and non-monotonic relationships between landscape changes and lake trophic dynamics.

In China, lakes serve as pivotal drinking water sources,[21] and their trophic states are predominantly affected by basin landscape transformations.[22] Roughly 60% of monitored Chinese lakes and reservoirs were eutrophic.[23] Approximately 80% of lakes in the Lower Yangtze River Basin—the largest freshwater lake cluster in China—were severely degraded due to nutrient accumulation.[24] Recurrent algal blooms in Taihu Lake compromised drinking water provision for over two million people.[12] This deterioration was linked to the most dramatic landscape transformations worldwide, particularly the urban sprawl and cropland intensification encroaching upon woodlands and wetlands.[25,26] Landscape patterns and their trajectories vary markedly across China: southeast of the Hu-line concentrated around 95% of monsoon cropland and urban area,[27] whereas northwestern regions (e.g., Tibetan Plateau, Xinjiang) have experienced greater ecological disturbance in recent decades.[28] Although recent studies have mapped lake trophic indices[4,29] and explored their general responses to climatic and anthropogenic pressures,[22] they rely on a single water quality indicator or a proxy index retrieved from remote sensing images. While computationally efficient, such 'black-box' retrieval of composite indices often masks the nuanced responses of individual trophic indicators (e.g., chlorophyll-a, Chl-a; total phosphorus, TP, and Secchi disk depth, SDD) to basin landscape transformations, obscuring the underlying mechanisms. Further, alternative pathways for socioeconomic development are expected to amplify the spatiotemporal variations in lake trophic states under climatic crisis.[3] A predictive perspective is still lacking at China's national scale, impeding sustainable planning and targeted lake ecosystem management across regions.

Landscape pattern metrics (LPM) have been widely adopted to precisely quantify landscapes from the perspectives of diversity, fragmentation, shape, zonality, etc.[30] The comprehensive trophic level index (TLI) has been officially adopted to assess eutrophication status by synthesizing multiple water quality parameters.[31] A wide spectrum of techniques, such as geographically weighted regression, redundancy analysis, and stepwise linear regression (SLR), have been used to advance understanding of landscape-water quality interactions.[32,33] Nevertheless, the increasing availability of metrics has introduced issues such as autocorrelation, redundancy, and overfitting.[14] Data-driven machine learning (ML) algorithms, such as Random Forest (RF) and Artificial Neural Network (ANN),[18,34] offer new opportunities for addressing the complex, non-linear interactions and large predictor sets.[35,36] Moreover, advances in remote sensing (RS) now enable large-scale, long-term water quality monitoring, facilitating effective ML training. Post-hoc explanation techniques (e.g., SHapley Additive exPlanations, SHAP) are expected to improve ML model interpretability,[37] enabling identification of dominant LPMs and potential thresholds in their influence on lake trophic states.

Here, we investigate landscape-driven variations in lake trophic states across different regions in China employing explainable ML algorithms (Figure 1). Specifically, our objectives are to: (1) characterize historical spatiotemporal changes in landscape and multi-indicator trophic state (i.e., TLI) of lakes across regions; (2) identify nonlinear relationships and critical thresholds between LPMs and lake trophic state changes, by comparing performances of SLR, RF, ANN, and deep neural networks (DNN); and (3) project future TLI trajectories under alternative RCP scenarios to inform

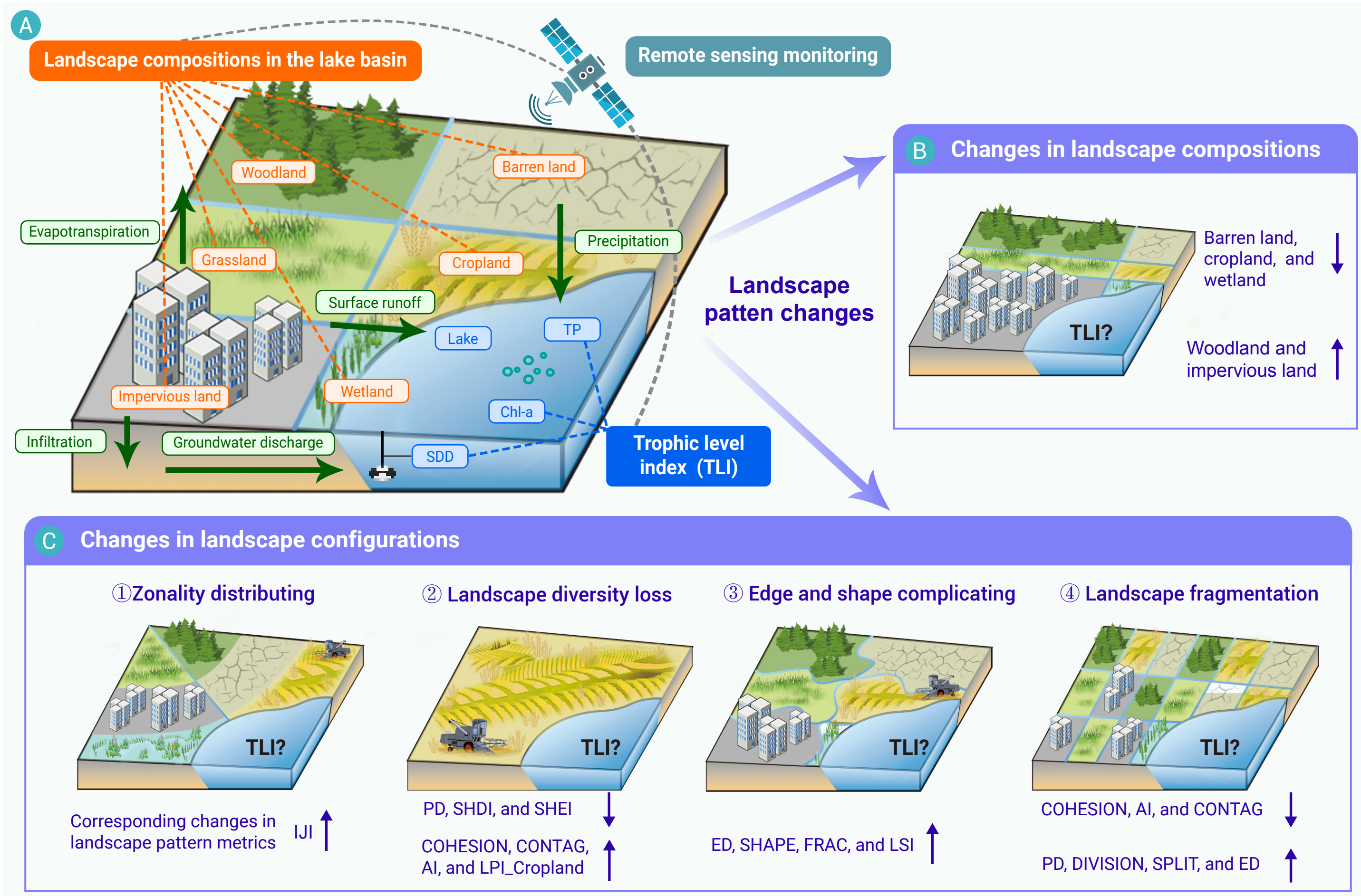

Figure 1. Conceptual diagram illustrating how landscape transformations influence lake trophic states National-scale spatiotemporal dynamics in landscape patterns and lake trophic states were quantified using remote sensing datasets.

tailored strategies for protecting water quality and optimizing synergies in water-food-energy nexus.

MATERIALS AND METHODS

Study area

China is characterized by highly heterogeneous landscape patterns and has undergone rapid land-use transitions over recent decades.[38] Lakes in China span diverse climatic and physiographic regions and are commonly categorized into six limnetic zones,[39] namely the Northeast Plain and Mountains (NE), Eastern Plain (EP), Yunnan-Guizhou Plateau (YG), Inner-Mongolia Plateau (MP), Tibetan Plateau (TB), and Xinjiang (XJ) (Figure 2). A total of 443 lakes over 20 km^2 are involved in this study, of which 282 are located in TB, 73 in EP, 36 in XJ, 23 in NE, 18 in MP, and 11 in YG.

Data preparation and preprocessing

Accurate locations and areas of lakes were obtained from the China Lake Dataset 2020.[40] We focused on the catchment scale, as nutrients received by lakes are governed by cumulative hydrological and ecological processes operating across the entire catchment, including surface runoff, infiltration, and subsurface flow (Figure 1). Limiting analysis to a fixed buffer scale may overlook upstream landscape transformations that substantially contribute to nutrient loading, especially in large basins. Despite the scale effects, recent studies demonstrated that the impacts of landscape patterns on water quality were equally critical at the riparian zone and catchment scale.[41] Lake basin boundaries were obtained either from the Lake-Watershed Science Data Center[42] or outlined by ArcSWAT, based on a digital elevation model (DEM) from GEBCO Compilation Group.[43]

Basin landscape patterns were characterized using land use/land cover data, herein China's Land-Use/Cover Datasets (CLUD) with a 30m resolution from 2000 to 2020.[27] We focused on the landscape composition with significant impacts on water quality, as suggested in previous studies,[17,41] namely cropland, woodland, grassland, barren land, impervious land, and wetland. The lake area was considered as an auxiliary landscape feature. LPMs impact the ecological process at three levels—patches, classes, and entire landscape mosaics.[14] Given that the patch level was too fine-grained for explaining the overall relationships, we calculated nine metrics at the class level and 14 at the landscape level (Table 1). These metrics have been proven to be significantly correlated with nutrient loading. LPMs were computed within delineated lake basin boundaries for 2000, 2005, 2010, 2015, and 2020 using categorical map CLUD via FRAGSTATS v4.2 software,[44] adhering to 8-cell neighborhood rules. Detailed descriptions and formulations of LPMs are available in Table S1.

Lake trophic states were assessed by comprehensive trophic level index (TLI), an empirical Chinese adaptation of Carlson's trophic state index that integrates TP, Chl-a, and SDD.[31] TP, Chl-a, and SDD data for 2000-2020 were derived from our previously published RS retrievals: TP was mapped by Fang et al. using MOD09GA/MYD09GA and MOD09GQ/MYD09GQ images;[45] Chl-a was mapped by Li et al. using Sentinel-2 MSI imagery;[46] SDD was mapped by Liu et al. using MOD09GA images.[47] The RS retrievals of TP, Chl-a, and SDD are subject to several sources of uncertainty, including sensor noise, atmospheric correction residuals, and optical complexity of inland waters. These uncertainties are inherent to large-scale remote sensing products and were not explicitly corrected in this study (see accuracy for each dataset in Table S2). To quantify error propagation from RS products to the final TLI, Monte Carlo simulations (n = 1,000) were implemented by perturbing Chl-a, TP, and SDD using their reported RMSE values for each lake. The propagated uncertainty resulted in a mean TLI standard deviation of 8.67, corresponding to 17% of the mean value (Figure S1). Although total nitrogen (TN) is also a recognized limiting factor,[31] especially in subtropical and plateau shallow lakes,[48] it was excluded from this calculation due to the lack of robust, long-

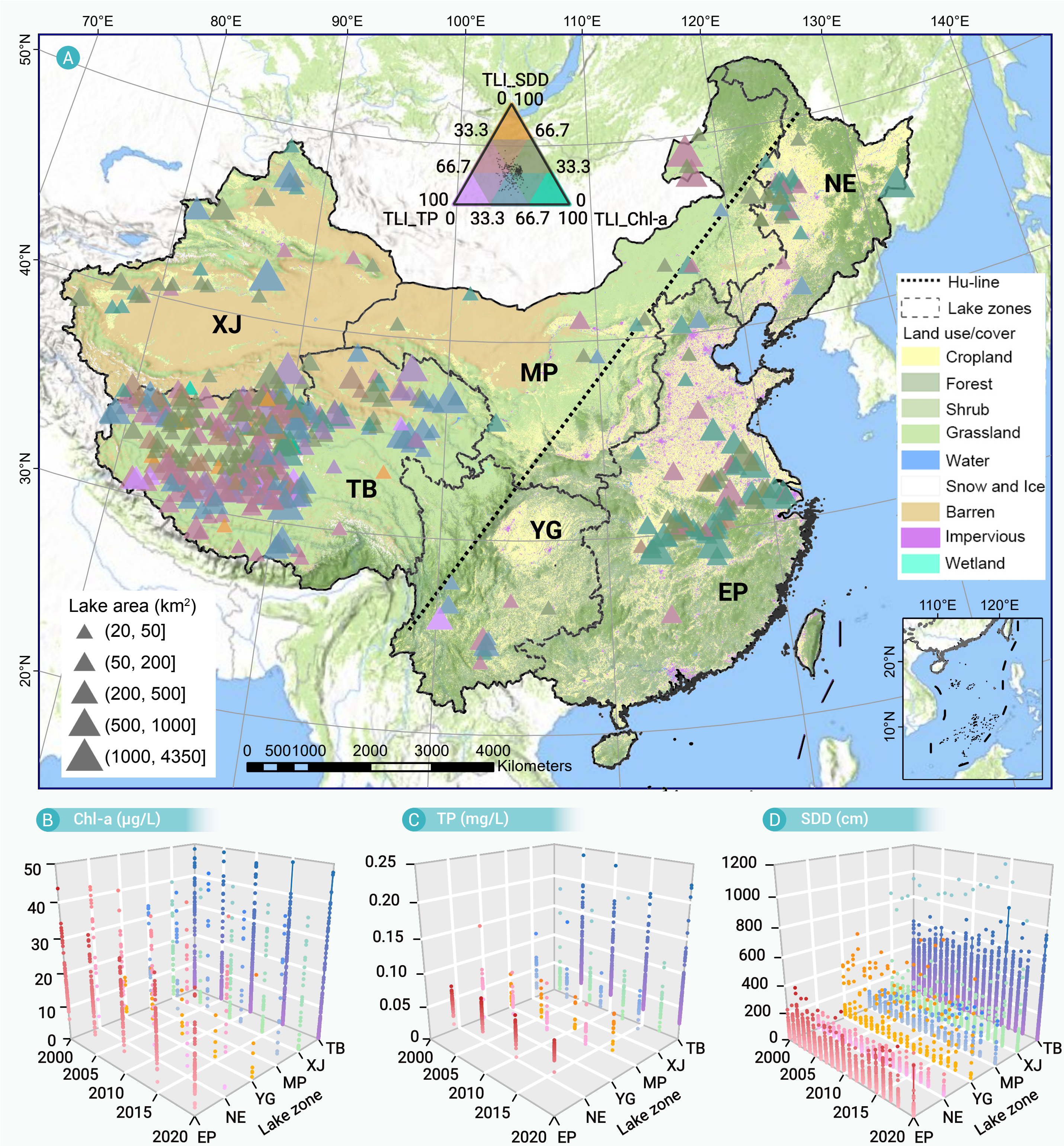

Figure 2. Spatial distribution and trophic characteristics of 443 Chinese lakes (> 20 km^2) (A) Ternary choropleth map showing lake distributions and the relative contribution of Chl-a, TP, and SDD to the comprehensive TLI. Colors encode the relative proportions of the three indicators according to the ternary legend. Lakes are grouped into six limnetic zones: Northeast Plain and Mountain (NE), Eastern Plain (EP), Yunnan-Guizhou Plateau (YG), Inner-Mongolia Plateau (MP), Tibetan Plateau (TB), and Xinjiang (XJ). (B–D) Temporal variations in Chl-a (B), TP (C), and SDD (D) from 2000 to 2020. Colors distinguish limnetic zones, and color gradients indicate the magnitude of each trophic indicator.

term, and spatially consistent RS products at the national scale. Therefore, the TLI framework here follows the conventional three-parameter Carlson Index and reflects a phosphorus-focused trophic assessment, which is commonly applied in RS-based lake trophic status estimation.[4] According to TLI, lakes were categorized into five classes, namely oligotrophic (TLI < 30), mesotrophic (30 ≤ TLI < 50), light eutrophic (50 ≤ TLI < 60), middle eutrophic (60 ≤ TLI < 70), and hyper eutrophic (TLI > 70).

For each of the three indicators, the average value of all pixels within each lake boundary was computed for the year to reduce random errors from pixel-level noise and temporal outliers, ensuring the reliability of multi-decadal trends. The yearly TLI was calculated as follows:

Table 1. Landscape Pattern Metrics (LPMs) employed in this study.

Level	LPMs	Abbreviation
Class	Area percentage of each landscape class within the basin	/
Class and Landscape	Largest patch index	LPI
	Edge density	ED
	Area-weighted mean shape index	SHAPE_AM
	Area-weighted mean fractal dimension index	FRAC_AM
	patch density	PD
	Landscape division index	DIVISION
	Splitting index	SPLIT
	Patch cohesion index	COHESION
Landscape	Landscape shape index	LSI
	Contagion index	CONTAG
	Aggregation index	AI
	Interspersion and juxtaposition index	IJI
	Shannon's diversity index	SHDI
	Shannon's evenness index	SHEI

$$TLI = \sum w_j \cdot TLI_j \tag{1}$$

$$w_j = \frac{r_j^2}{\sum_{j=1}^{3} r_j^2} \tag{2}$$

where TLI_j and w_j denote the trophic level index and its weight demonstrated by the jth indicator, and r_j is the national-average correlation coefficient between the jth indicator and Chl-a, as Chl-a is central to reflecting algal biomass. The calculation of TLI_j was with reference to equation (3)~(5).

$$TLI_{Chl-a} = 10\left(2.5 + 1.086 \ln Chl - a\right) \tag{3}$$

$$TLI_{SDD} = 10\left(5.118 - 1.94 \ln SDD\right) \tag{4}$$

$$TLI_{TP} = 10\left(9.436 + 1.624 \ln TP\right) \tag{5}$$

The conceptual diagram of the relationship between basin LPMs and lake TLI was illustrated in Figure 1.

Pearson correlation matrices were constructed to assess pairwise correlations among LPMs and between LPMs and trophic state indicators (Figure S2), evaluating potential multicollinearity among LPMs and exploring their associations with lake trophic status, respectively. Analyses of variance (F-test) were conducted to clarify the significance of interregional differences before regional modelling (Table S3).

Model development

Model optimization. To untangle the relationship between LPMs and TLI, we optimized SLR, RF, and Backpropagation Neural Networks (BPNN) algorithms. Backward elimination SLR is capable of reducing multicollinearity by automatically selecting the predictor subset with the lowest Akaike Information Criterion.[49] RF algorithm is a bagging-based ensemble ML method consisting of numerous decision trees.[50] We utilized Recursive Feature Elimination (RFE) with repeated cross-validation (RCV) to select predictive features fed into RF models via 'caret' package in R,[51] consequently reducing the risks of multicollinearity and model overfitting.[35] An automated hyperparameter tuning was employed to search for the optimal '*mtry*', with respect to Out-Of-Bag (OOB) error estimate[52]. Hyperparameter '*ntree*' was assigned to 500, which was verified as large enough to achieve convergence of OOB error for the sample size of this study. BPNN consists of interconnected neurons organized into an input layer, hidden layers, and an output layer. We constructed an artificial neural network (ANN) with a single hidden layer and a deep neural network (DNN) with two hidden layers,[37] as the computational cost with each additional hidden layer exponentially increase and two layers are sufficient for approximating any smooth mapping.[53] The number of neurons in hidden layers was determined as 15, which provided the best balance between goodness of fit and training efficiency, through a grid search optimization algorithm concerning Root Mean Square Error (RMSE) in RCV.[51] The logistic function served as the activation function in BPNN. The ML models (RF and BPNN) exhibit inherent robustness to outliers, thereby partially mitigating error propagation from RS datasets.

Performance comparison. The performances of SLR, RF, ANN, and DNN models at the national scale were tested on the held-out test data, 20% of the dataset, via model explainers in 'DALEX' package.[54] We assessed the model performance by illustrating the distribution of residuals and by calculating metrics including median absolute deviation (MAD), RMSE, and coefficient of determination (R^2) across five repeats of 10-fold RCV (Eq. (6)~(8)).

$$R^2 = 1 - \frac{\sum_i^n (\hat{y}_i - y_i)^2}{\sum_i^n (y_i - \bar{y})^2} \tag{6}$$

$$RSME = \sqrt{\frac{1}{n}\sum_i^n (\hat{y}_i - y_i)^2} \tag{7}$$

$$MAD = meadian\left(|\hat{y}_1 - y_1|, \ldots, |\hat{y}_n - y_n|\right) \tag{8}$$

where y_i is the actual observed value for the ith lake, $\bar{y}$ is the mean of all the observed values, and $\hat{y}_i$ is the predicted value for the ith lake.

Model explanation

Considering the model performance and efficiency (Figure S6), RF algorithm was implemented to develop separate models for LPMs-TLI relationships across six limnetic zones. To investigate the threshold effects, Partial Dependence Profiles (PDP) were generated for each model via 'DALEX' package.[54] PDP has been a mainstay for ecological and environmental inference, estimating the marginal effects of predictors as the average of a set of individual ceteris-paribus profiles.[36] Further, to ascertain the dominant predictors for TLI, SHapley Additive exPlanations (SHAP) feature importance was calculated for each model via the 'fastshap' package.[55] SHAP invoked the classic game-theoretic Shapley value to quantify the contribution of each feature to the prediction of each instance.[56] The number of Monte Carlo repetitions for estimating each SHAP value was 100 in this study.

Lake trophic state projection under future scenarios

We projected the lake TLI across six limnetic zones by 2100 along the storylines of landscape changes through alternative RCPs. Simulated 30m-resolution land use/cover for the years 2040, 2060, 2080, and 2100 were accessed for LPMs calculation under RCP2.6, RCP4.5, and RCP8.5,[57] assuming a low, medium, and high radiative forcing scenario,[58] respectively. Projected LPMs were thereby fed into the RF models to project future TLI. We assumed the extent of lakes would remain constant from 2020 to 2100 under alternative scenarios.

RESULTS AND DISCUSSION

Historical heterogeneity in landscape and eutrophication trends

In China, lake trophic states were significantly associated with basin landscape patterns ($p < 0.05$, Figure S2) and exhibited marked spatial heterogeneity across the six limnetic zones (Figures 2, S3 & Table S3). Eastern lakes (EP and NE) predominantly received runoff from cropland and impervious land, the area of which was ten times broader than that in western China (Figures 3D1 & E1), accompanied by higher population density and human activities.[59] By 2020, 93% of EP lakes and 91% of NE lakes were in eutrophic states (Figures 3D2 & E2), characterized by high Chl-a concentrations (Figures 2A & B). Lakes in NE exhibited the highest TLI (58.54±1.44), Chl-a (23.40±2.51 μg/L), and TP concentration (89.02±3.05 μg/L) after 2000 (Figure 2B), particularly in the Songnen Plain (Figure S3), where agricultural and industrial productions were intense.[60]

In northwestern China (MP and XJ), around 65% and 55% of lakes were eutrophic by 2020, with TLI as 56.05±2.10 and 51.44±2.07 (Figures 3A2 & B2). These lakes are characterized by low SDD together with elevated TP and Chl-a concentrations (Figure 2). The northwest is dominated by low-vegetation grassland and extensive barren land (over 20 times greater than the proportion in the east) (Figures 3A1 & B1), where wind and runoff could mobilize and deliver nutrients and sediments to lakes.[61]

Lakes in YG are concentrated in the mountainous basins dominated by woodlands (Figure 2A). Half of the lakes were mesotrophic in 2020 and displayed the highest SDD (214.48±59.24 cm) among lake zones (Figures 2D & 3F2), likely attributed to the greater depth of rifted lakes.[47] The TB, a grassland-dominated region, hosts a complex lake system (282 lakes) spanning oligotrophic (9% in 2020) to hyper-eutrophic (5% in 2020) states. Overall, TB witnessed the lowest mean TLI (43.68±0.82) in 2020, consistent with relatively low anthropogenic land exploitation and disturbance. Our TLI estimates constructed on remotely sensed Chl-a, TP, and SDD were consistent with the TSI-based remote assessments for China,[4,29] which exhibited a spatial disparity with the lowest eutrophic proportion in TB and the highest in EP.

Temporally, the lake trophic conditions have substantially improved from 2000 to 2020, as Chl-a and TP concentrations declined and SDD rose (Figure S4). The national proportion of eutrophic lakes fell from 69.07% to 44.24%; the number of hyper-eutrophic lakes decreased from 130 to 17 (Figure 3). These trends align with the long-term TSI trends reported by Hu et al.[4] and reflect the environmental cost of rapid urbanization, industrialization, and agricultural intensification before 2000 and the achievements after stepping into the post-2000 lake-catchment management stage.

Regional trajectories diverged. Thanks to the restoration projects, such as the Three North Shelterbelt Forest Program and the Grain for Green project,[62] barren land in the northwest (MP, XJ, TB) has declined by 1.38%, 2.39%, and 1.2% from 2000 to 2020 (Figures 3A1–C1). Simultaneously, average SDD in these zones increased by 32.97 cm (32%), 62.62 cm (59%), and 66.33 cm (77%), respectively (Figure 2C). Corresponding declines in mean TLI were substantial (MP, -5%; XJ, -20%; TB, -38%), indicating improved water clarity and reduced trophic pressure in massive northwestern lakes (Figure S3).

On the southeastern side of Hu-line (NE, EP, YG), basins have experienced a continued increase in impervious land at the expense of cropland between 2000 and 2020 (Figures 3D1–F1). The EP, particularly the lower Yangtze River basin, has undergone the greatest urbanization (+5% impervious land) (Figure 3E1), consistent with population concentration and rapid socioeconomic development.[59] This trend was associated with a 4.80 μg/L (6%) TP elevation. In YG, 2.86% impervious land expansion, 7.51 μg/L (10%) TP elevation, and 1.37 μg/L (17%) Chl-a elevation occurred concurrently. Although the Grain for Green project in YG produced an 11% woodland gain by converting cropland, these benefits have been offset by concurrent impervious-surface expansion and nutrient increases, since mean TLI declined marginally since 2000 (-2%).

Taken together, these results suggest that the national improvement in the 21st century demonstrated strong interregional heterogeneity: northwestern regions generally experienced clearer water and lower trophic indices following restoration-driven green gains, whereas southeastern regions continue to face nutrient pressures associated with urbanization and cropland intensification. The underlying trends of Chl-a, TP, and SDD behind TLI and associated basin landscape dynamics were even more inconsistent across regions. Policy and management should therefore account for such regional contrasts and prevent giving one-sided credence to the national-scale TLI trends while overlooking localized latent water-quality threats (e.g., elevated TP in EP and YG). The neglect could lead to inefficient resource allocation, aborted ecological restoration efforts, and consequent outbreaks of algal blooms under future warming.

Divergent landscape–trophic state coupling mechanisms

To unravel the dominant LPMs influencing lake trophic states across regions, TLI, Chl-a, TP, and SDD were modeled using the optimized RF framework, which outperformed SLR, ANN, and DNN algorithms in predictive performance (for a detailed performance comparison, see Figure S5). Our results demonstrated that LPMs dominated lake trophic state variations, explaining 43.88% (EP) to 70.05% (YG) of TLI variance, 32.44% (TB) to 80.34% (YG) of Chl-a variance, 30.51% (EP) to 73.74% (YG) of TP variance, and 47.29% (EP) to 74.2% (YG) of SDD variance. Overall, landscape pattern changes exerted the greatest impact in YG and the weakest in EP.

Regional contrasts reflected divergent geomorphology and pollutant pathways. In YG, many lakes are situated in karst-dominated, steep basins characterized by strong subsurface connectivity and rapid overland flow. Such geomorphic conditions reduce nutrient retention in soils and accelerate the transfer of pollutants from hillslopes to lakes.[63] Deep-water, rifted morphologies and limited macrophyte coverage further constrain in-lake nutrient assimilation,[47,64] thereby amplifying sensitivity to landscape disturbance. Conversely, in the densely populated EP, the lower explanatory power likely reflects the dominance of external point-source pollution (e.g., municipal and industrial sewage, aquaculture discharge) that mask the influence of landscape processes.[12,65]

Lake area consistently emerged as a key predictor, reflecting its control over water volume, residence time, and solute dilution capacity (Figure 4). Beyond area, the dominant LPMs and their functional thresholds revealed distinct regional mechanisms.

In southeastern China (EP, NE, YG), anthropogenic landscape metrics were the dominant predictors of trophic states. In the highly urbanized EP, nonlinear responses to impervious patch density (PD) indicated a fragmentation effect: as PD exceeded 5 patch ha^{-1}, the discrete patches created a capillary-like network that substantially increased the interface for pollutant transport, raising TLI from 55 to 62, elevating Chl-a by 15%, and reducing SDD by 58% (Figures 4A, S6 & S8). Such patterns support limiting patch proliferation in urban planning.[66] In YG, the complexity of impervious edges (FRAC/SHAPE) was the primary driver, explaining 46.63% of TLI variations (Figure 4C). Increasing impervious FRAC from 1 to 1.3 raised TLI from 45 to 53, elevated TP by 15%, and decreased SDD by 20% (Figures S7 & S8), indicating the edge complexity increased hydrological connectivity and delivery efficiency relative to area. Despite YG having a smaller absolute urban footprint than EP (Figure 3), complex basin topography and longer hydraulic residence times potentially exert disproportionate impacts per unit of impervious area.[67] In NE, wetland and woodland functioned as primary nutrient sinks. Increased wetland edge density (ED) increased TLI primarily by reducing SDD (Figures 4B & S8), likely due to the degradation of wetland fringes. Greater woodland coverage improved SDD and decreased Chl-a by enhancing deten-

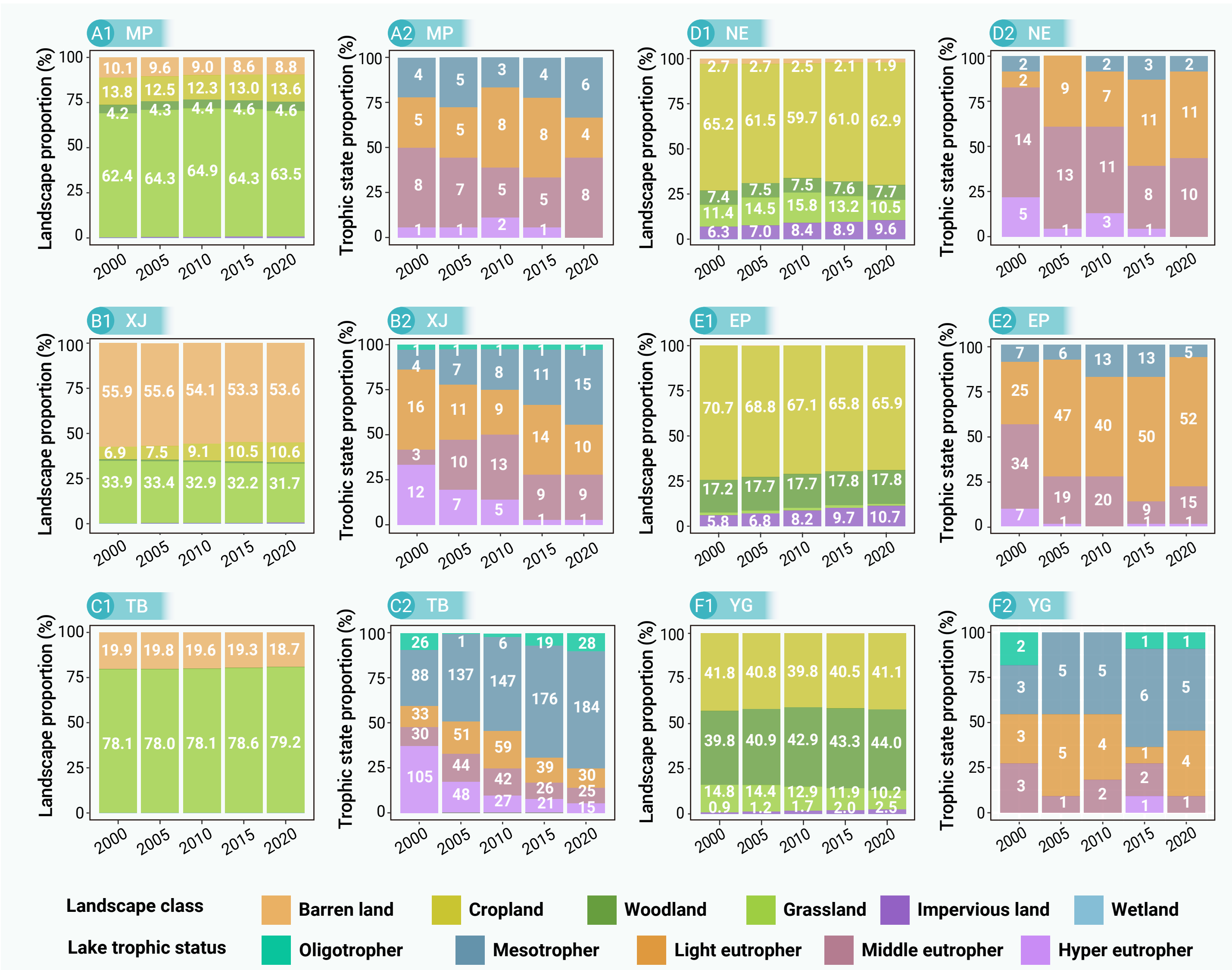

Figure 3. Temporal variations in basin landscape composition and lake trophic state across six limnetic zones (2000-2020) For each zone, the left panels (A1–F1) show proportional coverage (%) of major land-cover classes within lake catchments, with percentages labeled inside. The right panels (A2–F2) show the proportions of lakes in each trophic category, with lake numbers labeled inside the bars. (A) Inner-Mongolia Plateau (MP); (B) Xinjiang (XJ); (C) Tibetan Plateau (TB); (D) Northeast Plain and Mountain (NE); (E) Eastern Plain (EP); (F) Yunnan-Guizhou Plateau (YG).

tion and nutrient absorption (Figures S6 & S8).

In northwestern China, natural-land metrics dominated trophic dynamics. In MP, the woodland LPI, which reflects the integrity of core woodland patches, had the strongest influence. Increasing LPI from 0 to 1% reduced TLI from 58 to 54, decreased Chl-a by 12%, and raised SDD by 10% (Figure 4D), indicating that large contiguous forest patches in MP promoted soil stabilization, improved buffer-strip continuity, and increased contaminant retention. In contrast, fragmented woodland patches (high SPLIT values) provided limited buffering against nutrient loading. In XJ, different LPMs affected distinct trophic components: cropland coverage predominantly affected TP, reflecting agricultural nutrient sources; grassland LPI primarily affected SDD, likely via erosion control and sediment regulation; woodland and barren-land fragmentation strongly influenced Chl-a, likely due to intensification of both wind and water erosion caused by edge effects. These multi-pathway interactions necessitate integrated, multi-target management interventions for XJ. In TB, TLI responses to landscape zonality (IJI) suggest that ecological corridor connectivity and landscape interspersion in montane-zonal structures may enhance ecosystem resilience,[68] reducing TLI from 52 (eutrophic) to 48 (mesotrophic) as IJI increased from 0 to 20%. The stronger natural sensitivity observed on the Hu Line's northwestern flank concurs with Kong et al.,[28] indicating that landscape transformation produces more severe ecological consequences in the northeast than in the southeast.

Future trajectories of lake trophic state and the implications

Projected socioeconomic pathways generate different land-use trajectories across regions that produce region-specific responses of lake trophic state (Figures 5-6). Among scenarios, YG lakes were consistently forecast to face severe trophic state degradation, although other zones show variable responses (Figures 5A, C & S8).

At the national scale, the mean TLI for the 443 lakes would increase from 47.83 (2020) to 49.90 under RCP2.6, to 49.72 under RCP4.5, and to 49.61 under RCP8.5 (Figure 5A) by 2100. The relatively larger rise under RCP2.6 is counterintuitive since RCP2.6 represents an environmentally friendly pathway that aims to curb urbanization, fossil fuel use, and meat consumption to limit global warming below 2°C.[58] This pattern primarily resulted from projected agricultural expansion for food and biofuel demands, which increases cropland area and edge density in basins and therefore substantially declines SDD (Figures 5B, S8 & S9). In YG, for example, cropland coverage was projected to grow by 6%, and cropland ED rose from 35 to 50 m ha^{-1}, inducing a 30% decrease in SDD (Figure S9) and a 5.4% increase in mean TLI (Figure 5C2). In XJ, projected cropland expansion of 2.5% (replacing grassland), together with a 2% increase in cropland LPI and 1% decline in grassland LPI, would drive a 4% SDD decline, a 0.7% TP increase, and a 0.5% Chl-a increase (Figure S9), yielding a 0.7% TLI elevation (Figures 4C3 & S10). In TB, barren land fragmentation was projected to be the crux of modest trophic

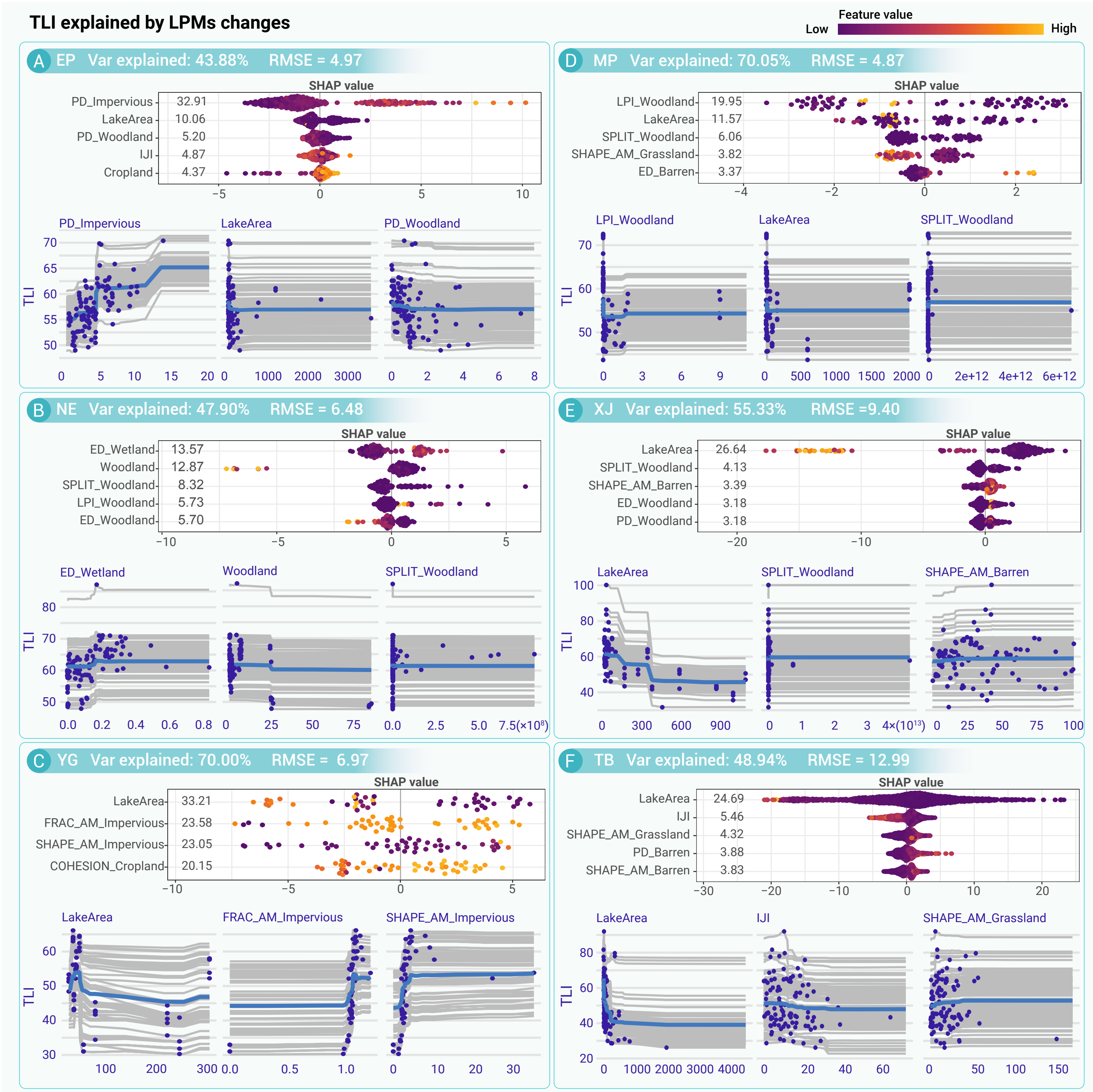

Figure 4. SHAP- and PDP-based interpretation of landscape controls on lake trophic state across six limnetic zones (2000-2020) The upper panels in each block exhibit SHAP value distributions for the five most influential landscape metrics ranked by mean absolute SHAP values, with their relative contributions (%) annotated alongside. The lower panels in each block exhibit the partial dependence profiles (PDPs) for the three most influential metrics. Grey lines show individual ceteris-paribus profiles for 100 randomly selected observations, and blue lines represent the corresponding PDPs. Additional interpretations for the Chl-a, TP, and SDD models are provided in Figures S6-S8. EP, Eastern Plain; NE, Northeast Plain and Mountain; YG, Yunnan-Guizhou Plateau; MP, Inner-Mongolia Plateau; XJ, Xinjiang; TB, Tibetan Plateau.

state degradation (Figure S10).

The counterintuitive response under RCP2.6 highlights a broader water–food–energy (WFE) dilemma. Climate mitigation pathways that rely on land-based solutions, including bioenergy expansion and natural landscape reclamation, may unintentionally intensify nutrient output and increase eutrophication risks. (Figure 5A1). Bioenergy expansion under RCP2.6 has been evidenced to bring about greater nitrogen loads in river systems.[69] Along with *Wetland International*'s campaign against the loss of wetlands for biofuel production,[70] coordinated nutrient management, precision agriculture, and buffer-zone restoration would be required to offset the water-quality risks associated with bioenergy-based mitigation strategies. These findings highlight that climate mitigation policies should be evaluated not only in terms of carbon outcomes but also through their cascading impacts on WFE nexus. Decision-making and long-term planning should highlight these cross-sectoral interactions, integrating water-security objectives into national strategies towards Sustainable Development Goals.[71]

Under RCP4.5, where the target is to stabilize radiative forcing through coordinated management and policies (e.g., improving single-yield on cropland and clean energy share),[72] northwestern lakes were expected to remain stable, while southeastern lakes (notably YG and NE) would experience more

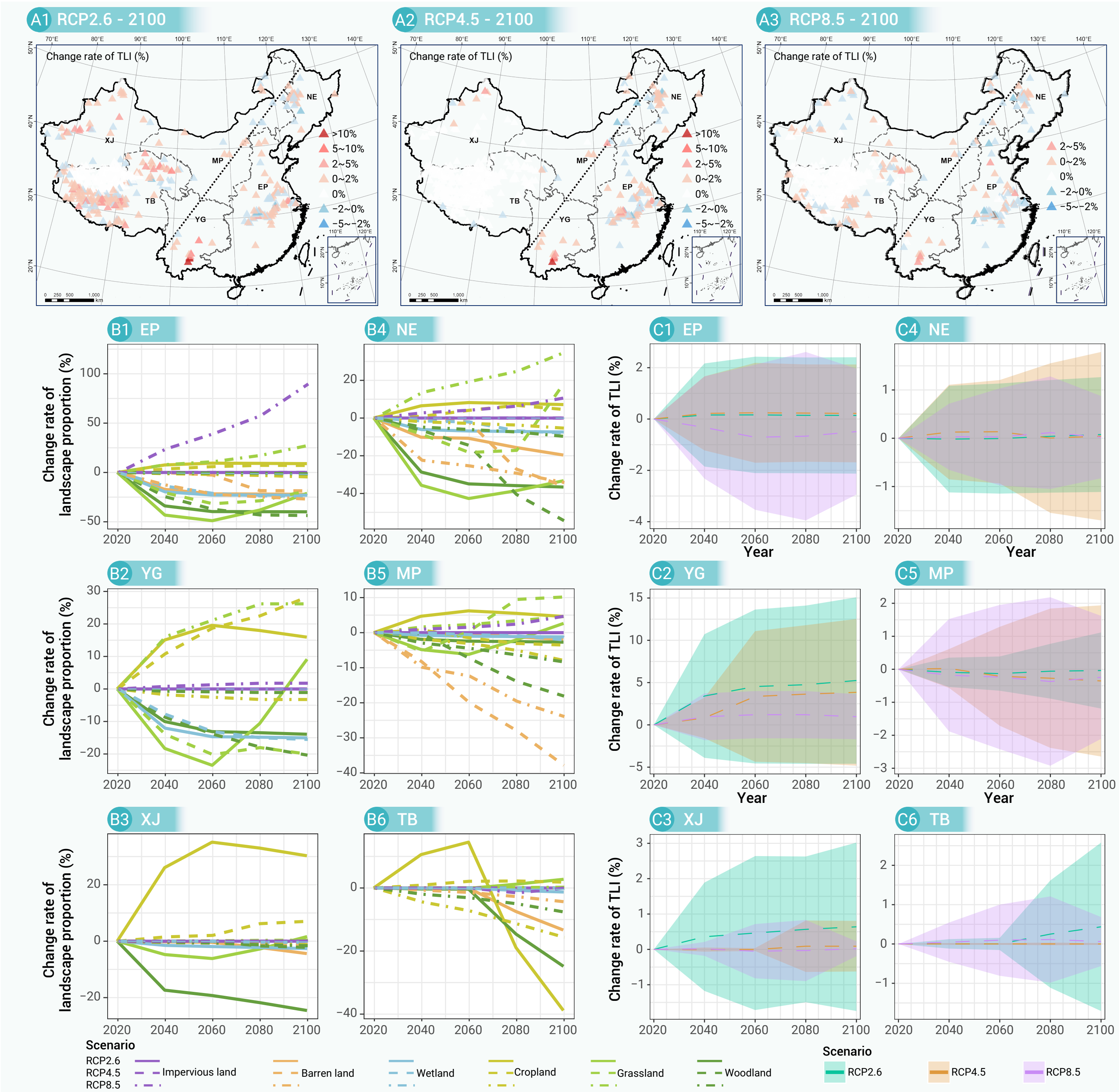

Figure 5. Projected trajectories of lake trophic state and basin landscape composition under RCP2.6, RCP4.5, and RCP8.5 (A1–A3) Spatial patterns of projected TLI change (%) for 443 lakes between 2020 and 2100 under each scenario. (B1–B6) Temporal changes in basin landscape composition across the limnetic zones, expressed as percentage change relative to 2020. (C1–C6) Corresponding projected changes in TLI. EP, Eastern Plain; NE, Northeast Plain and Mountain; YG, Yunnan-Guizhou Plateau; MP, Inner-Mongolia Plateau; XJ, Xinjiang; TB, Tibetan Plateau.

marked changes (Figures 5A2 & 6A2–C2). In YG, RCP4.5 projected a 10% increase in cropland coverage and a 4 m ha^{-1} increase in its ED (Figure S10). In NE, lake trophic pressure (especially in Chl-a) would primarily come from woodland shrinkage (Figures 4B, 5B4 & 6A2), as converting woodlands to energy crops was considered the cost-minimizing pathway to radiative stabilization under RCP4.5.[72] This shortcut reduced woodland cover from 7.3% to 5.9% and its ED from 2.5 to 2.0 m ha^{-1} (Figure S10), driving a small (1%) Chl-a elevation (Figure S8). The deterioration in Chl-a should not be ignored, although SDD gains offset this effect and moderated TLI (Figures 5C4 & S9), because NE already exhibited the highest Chl-a levels in 2020 (Figure 2C). Projected surges in temperature and precipitation in NE,[73] which are likely to disrupt freeze-thaw cycles and escalate surface runoff, would further exacerbate water-security inequalities between NE and other regions. Although some restorative initiatives might be implemented after 2080, when 3% of grassland would recover from cropland (Figure 5B4), the Chl-a showed limited response (Figure 5A2). These findings underline the necessity of targeted measures in accordance with localized crux in eutrophic problems to avoid inefficient efforts.

Under RCP8.5, a high-development pathway with hands-off resource exploitation, trophic trajectories of lakes demonstrated the strongest spatial unevenness (Figures 5 & 6). Some highly urbanized areas in EP, particularly the middle and lower Yangtze Plain, were projected to show improvements in water clarity (+5.7% SDD) and declines in Chl-a (-2.9%), yielding a 0.5% TLI decline (Figures 5 & S9). These improvements were attributed to spatial

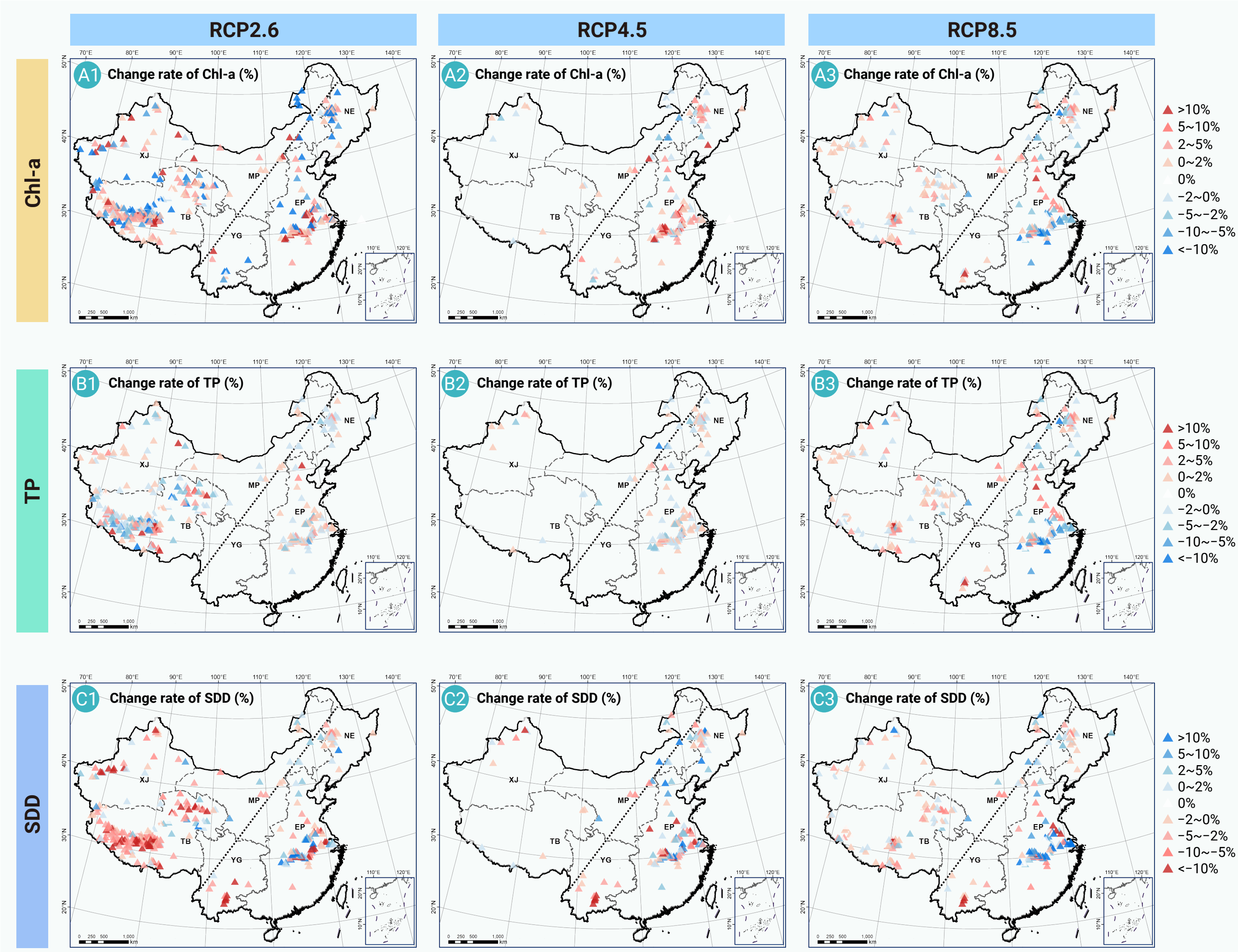

Figure 6. Projected trajectories of Chl-a (A1–A3), TP(B1–B3), and SDD(C1–C3) under RCP2.6, RCP4.5, and RCP8.5 Spatial patterns of projected changes (%) in Chl-a, TP, and SDD for 443 lakes between 2020 and 2100 under each scenario, expressed as percentage change relative to 2020. EP: Eastern Plain; NE: Northeast Plain and Mountain; YG: Yunnan-Guizhou Plateau; MP: Inner-Mongolia Plateau; XJ: Xinjiang; TB: Tibetan Plateau.

aggregation of impervious surfaces during the high-degree urbanization and relocated agricultural activities (Figure S9). Conversely, YG was projected to suffer from irregular urban sprawl (a concurrent increase in impervious LPI and SHAPE), with estimated +3.8% in Chl-a and +2.4% in TP (Figure S9). These deteriorations in YG could be even stronger, considering the hilly terrain and heavier precipitation under RCP8.5.[73] Similarly, Ji et al. predicted a 25% rise in TP concentration in YG lake sediments by 2100 under RCP8.5.[67] The divergent trajectories between EP and YG emphasized the aggravated regional inequality in the future and necessitated technology and expertise transfer from high- to low-income regions.

It is noteworthy that the apparent improvement in EP under RCP8.5 is an artefact of modeled land-use shifts (e.g., near-complete urbanization) and should not be interpreted as a robust ecological benefit. Other pressures not fully captured by these landscape-pattern-only projections include increasing nitrogen inputs, elevated water withdrawals, and more frequent algal blooms owing to higher temperatures.[71,58] Therefore, even if high-emission RCP8.5 does not produce the worst modeled eutrophication or biodiversity loss,[74] achieving sustainable outcomes will still require proactive interventions in population growth, urban expansion, and climate change.

Limitations and Future Directions

Our ML-based multi-scenario projections provide a framework for national land planning under climate-policy pathways, while offering transferable lessons for other countries. Our projections isolated landscape-pattern effects and held other drivers (e.g., lake area and volume, future climatic conditions, point-source pollution controls, changes in wastewater treatment technologies) constant. This simplification was necessary to control the variables; however, substantial environmental and political changes have been altering trophic status of lakes. For instance, lake expansion in TB and XJ,[75,76] driven by glacier melt and increased precipitation, may induce a dilution effect that could partially offset landscape-driven trophic degradation. Warmer climates elevate lake temperature, thereby accelerating phytoplankton metabolism and extending the growing season.[73] In addition, management interventions represent another critical factor shaping projections. The large-scale governmental initiatives centered on the general national development strategy of "Ecological Civilization",[77] such as the "Water Pollution Prevention and Control Action Plan" and the "River and Lake Chief System", have substantially strengthened nutrient management and landscape restoration efforts. Consequently, evolving interventions could counterbalance the landscape-driven eutrophication risks projected here. Integrating land-use scenarios with dynamic climate projections and political factors, as well as their synergistic and antagonistic effects, represents an important direction for future research.

It should be noted that the TLI framework adopted in this study assumes phosphorus-limitation-centered trophic states and does not explicitly account for nitrogen limitation or N–P co-limitation. In lakes where nitrogen availability constrains primary production, especially in shallow lakes,[48] TLI-based trophic classifications and projected trends may reflect biases. Future work should incorporate TN and nutrient ratio (N:P), as well as other non-optically active water quality parameters (e.g., dissolved oxygen and chemical oxygen demand), to enrich the insights into lake trophic states when reliable large-scale RS products become available. Furthermore, while utilizing pre-validated RS products provides a consistent national baseline, we acknowledge that uncertainties in retrieval processes inevitably propagate through the models and may influence both historical estimates and scenario-based projections of lake TLI. Particularly, systematic biases could be introduced by errors in TP estimation due to over-correction of atmospheric effects in the clear lakes of the Tibetan Plateau,[45] as well as errors in TLI calculation arising from the fact that algal biomass in these oligotrophic lakes is more limited by nitrogen than by phosphorus.[48]

Integrating ML algorithms with theory- or process-based models offers a promising path to combine predictive accuracy with mechanistic understanding for more robust forecasts. This is particularly important in YG, where karst topography induces strong subterranean drainage and significantly mediates nutrient transport, explicitly incorporating hydrological models considering groundwater connectivity and subsurface nutrient transport processes would improve mechanistic interpretability and reduce potential bias.

CONCLUSION

This study developed an explainable random forest framework, which outperformed stepwise regression models and backpropagation neural network models, to unravel the nonlinear responses of lake trophic states to basin landscape pattern changes in China. We identified pronounced interregional unevenness in landscape-driven historical (pre-2020) and future (2020-2100) comprehensive trophic level index (TLI) of 443 lakes at the national scale, highlighting the differential roles of Chl-a, TP, and SDD. The national eutrophic proportion (TLI > 50) declined from 69.07% to 44.24% over the past two decades, with northwestern lakes benefiting from improved SDD associated with barren land reduction, while southeastern lakes faced rising Chl-a and TP linked to impervious land expansion. Key landscape controls varied regionally: natural landscape integrity (e.g., woodland largest patch index in Inner-Mongolia Plateau) primarily governed northwestern trophic states, whereas anthropogenic landscape dispersion and complexity (e.g., impervious patch density in Eastern Plain) disproportionately degraded southeastern lakes. Multi-RCP projections indicated that even sustainable pathways (RCP2.6 and RCP4.5) may not foster lake trophic state improvement if cropland expands and woodland is cleared for biofuel, while RCP8.5 would exacerbate interregional water security inequalities due to the spatially uneven urbanization. Localized, adaptive land-use strategies balancing food and energy demands with lake ecosystem resilience are critical for sustainable water management. Further interdisciplinary research incorporating hydrological processes and advanced remote sensing will be crucial in improving future projections.

REFERENCES

1. Messager M. L., Lehner B., Grill G., et al. (2016). Estimating the volume and age of water stored in global lakes using a geo-statistical approach. *Nat. Commun.* **7**:13603. DOI:10.1038/ncomms13603
2. Bakker K. (2012). Water security: Research challenges and opportunities. *Science* **337**:914–915. DOI:10.1126/science.1226337
3. Sinha E., Michalak A. M., Calvin K. V., et al. (2019). Societal decisions about climate mitigation will have dramatic impacts on eutrophication in the 21st century. *Nat. Commun.* **10**:939. DOI:10.1038/s41467-019-08884-w
4. Hu M., Ma R., Xue K., et al. (2024). A dataset of trophic state index for nation-scale lakes in China from 40-year Landsat observations. *Sci. Data.* **11**:659. DOI:10.1038/s41597-024-03506-7
5. Chaplin-Kramer R., Hamel P., Sharp R., et al. (2016). Landscape configuration is the primary driver of impacts on water quality associated with agricultural expansion. *Environ. Res. Lett.* **11**:074012. DOI:10.1088/1748-9326/11/7/074012
6. Heino J., Alahuhta J., Bini L. M., et al. (2021). Lakes in the era of global change: Moving beyond single - lake thinking in maintaining biodiversity and ecosystem services. *Biol. Rev.* **96**:89–106. DOI:10.1111/brv.12647
7. Vasistha P. and Ganguly R. (2020). Water quality assessment of natural lakes and its importance: An overview. *Mater. Today: Proc.* **32**:544–552. DOI:10.1016/j.matpr.2020.02.092
8. Smol J. P. (2019). Under the radar: Long-term perspectives on ecological changes in lakes. *Proc. Biol. Sci.* **286**:20190834. DOI:10.1098/rspb.2019.0834
9. Huang S., Zhang K., Lin Q., et al. (2022). Abrupt ecological shifts of lakes during the Anthropocene. *Earth Sci. Rev.* **227**:103981. DOI:10.1016/j.earscirev.2022.103981
10. Jane S. F., Hansen G. J., Kraemer B. M., et al. (2021). Widespread deoxygenation of temperate lakes. *Nature* **594**:66–70. DOI:10.1038/s41586-021-03550-y
11. Vörösmarty C. J., McIntyre P. B., Gessner M. O., et al. (2010). Global threats to human water security and river biodiversity. *Nature* **467**:555–561. DOI:10.1038/nature09440
12. Guo L. (2007). Doing battle with the green monster of Taihu Lake. *Science* **317**:1166–1166. DOI:10.1126/science.317.5842.1166
13. Beaulieu J. J., DelSontro T. and Downing J. A. (2019). Eutrophication will increase methane emissions from lakes and impoundments during the 21st century. *Nat. Commun.* **10**:1375. DOI:10.1038/s41467-019-09100-5
14. Frazier A. E., & Kedron P. (2017). Landscape metrics: Past progress and future directions. *Curr. Landscape Ecol. Rep.* **2**:63–72. DOI:10.1007/s40823-017-0026-0
15. Paule-Mercado M. C., Rabaneda-Bueno R., Porcal P., et al. (2024). Climate and land use shape the water balance and water quality in selected European lakes. *Sci. Rep.* **14**:8049. DOI:10.1038/s41598-024-58401-3
16. Scanlon B. R., Reedy R. C., Stonestrom D. A., et al. (2005). Impact of land use and land cover change on groundwater recharge and quality in the southwestern US. *Glob. Change Biol.* **11**:1577–1593. DOI:10.1111/j.1365-2486.2005.01026.x
17. Wei W., Gao Y., Huang J., et al. (2020). Exploring the effect of basin land degradation on lake and reservoir water quality in China. *J. Cleaner Prod.* **268**:122249. DOI:10.1016/j.jclepro.2020.122249
18. Wang R., Kim J. H. and Li M. H. (2021). Predicting stream water quality under different urban development pattern scenarios with an explainable machine learning approach. *Sci. Total Environ.* **761**:144057. DOI:10.1016/j.scitotenv.2020.144057
19. Simpson I. M., Winston R. J. and Brooker M. R. (2022). Effects of land use, climate, and imperviousness on urban stormwater quality: A meta-analysis. *Sci. Total Environ.* **809**:152206. DOI:10.1016/j.scitotenv.2021.152206
20. Song Y., Song X. and Shao G. (2020). Response of water quality to landscape patterns in an urbanized watershed in Hangzhou, China. *Sustainability* **12**:5500. DOI:10.3390/su12145500
21. Zhou Y., Chen L., Zhou L., et al. (2023). Key factors driving dissolved organic matter composition and bioavailability in lakes situated along the Eastern Route of the South-to-North Water Diversion Project, China. *Water Res.* **233**:119782. DOI:10.1016/j.watres.2023.119782
22. Xie G., Zhang Y., Wang Q., et al. (2025). Multiple impacts of climate change and anthropogenic activities on lacustrine trophic state. *Glob. Change Biol.,* **31**:e70510. DOI:10.1111/gcb.70510
23. China National Environmental Monitoring Centre (CNEMC). (2023). National Surface Water Quality Report. Available at: https://www.cnemc.cn/jcbg/qgdbsszyb/202308/P020230826693677796005.pdf (Accessed: 3 April 2024)
24. Zhang K., Yang X., Kattel G., et al. (2018). Freshwater lake ecosystem shift caused by social-economic transitions in Yangtze River Basin over the past century. *Sci. Rep.* **8**:17146. DOI:10.1038/s41598-018-35482-5
25. Radwan T. M., Blackburn G. A., Whyatt J. D., et al. (2021). Global land cover trajectories and transitions. *Sci. Rep.* **11**:12814. DOI:10.1038/s41598-021-92256-2
26. Mao D., Wang Z., Wu J., et al. (2018). China's wetland loss to urban expansion. *Land Degrad. Dev.* **29**:2644–2657. DOI:10.1002/ldr.2939
27. Yang J. and Huang X. (2024). The 30 m annual land cover datasets and its dynamics in China from 1985 to 2023. *Zenodo. Earth Sys. Sci. Data.* DOI:10.5281/zenodo.12779975
28. Kong X., Fu M., Zhao X., et al. (2022). Ecological effects of land-use change on two sides of the Hu Huanyong Line in China. *Land Use Policy* **113**:105895. DOI:10.1016/j.landusepol.2021.105895
29. Li S., Xu S., Song K., et al. (2023). Remote quantification of the trophic status of Chinese lakes. *Hydrol. Earth Syst. Sci.* **27**:3581–3599. DOI:10.5194/hess-27-3581-2023
30. Martinuzzi S., Januchowski-Hartley S.R., Pracheil B.M., et al. (2014), Threats and opportunities for freshwater conservation under future land use change scenarios in the United States. *Glob. Change Biol.* **20**: 113-124. DOI:10.1111/gcb.12383
31. China National Environmental Monitoring Centre (2026). National Surface Water Quality Report. Available at: https://www.cnemc.cn/jcbg/qgdbsszyb/202606/P020260625576645158655.pdf (Accessed: 21 July 2026)
32. Yu D., Shi P., Liu Y., et al. (2013). Detecting land use-water quality relationships from the viewpoint of ecological restoration in an urban area. *Ecol. Eng.* **53**:205–216. DOI:10.1016/j.ecoleng.2012.12.045
33. Peng S. and Li S. (2021). Scale relationship between landscape pattern and water quality in different pollution source areas: A case study of the Fuxian Lake watershed, China. *Ecol. Indic.* **121**:107136. DOI:10.1016/j.ecolind.2020.107136
34. Venkateswarlu T., Anmala J. and Dharwa M. (2020). PCA, CCA, and ANN modeling of climate and land-use effects on stream water quality of Karst watershed in Upper Green River, Kentucky. *J. Hydrol. Eng.* **25**:05020008. DOI:10.1061/(ASCE)HE.1943-5584.00019
35. Merghadi A., Yunus A. P., Dou J., et al. (2020). Machine learning methods for landslide susceptibility studies: A comparative overview of algorithm performance. *Earth Sci.*

Rev. 207:103225. DOI:10.1016/j.earscirev.2020.103225
36. Yu Q., Ji W., Prihodko L., et al. (2021). Study becomes insight: Ecological learning from machine learning. *Methods Ecol. Evol.* 12:2117–2128. DOI:10.1111/2041-210X.13686
37. Pichler M. and Hartig F. (2023). Machine learning and deep learning—A review for ecologists. *Methods Ecol. Evol.* 14:994–1016. DOI:10.1111/2041-210X.14061
38. Wei Y., Li H. and Yue W. (2017). Urban land expansion and regional inequality in transitional China. *Landscape Urban Plann.* 163:17–31. DOI:10.1016/j.landurbplan.2017.02.019
39. Zhang G., Yao T., Chen W., et al. (2019). Regional differences of lake evolution across China during 1960s–2015 and its natural and anthropogenic causes. *Remote Sens. Environ.* 221:386–404. DOI:10.1016/j.rse.2018.11.038
40. Zhang G. (2019). China lake dataset (1960s-2020). *National Tibetan Plateau / Third Pole Environment Data Center.* DOI:10.11888/Hydro.tpdc.270302
41. Shi X., Mao D., Song K., et al. (2024). Effects of landscape changes on water quality: A global meta-analysis. *Water Res.* 260:121946. DOI:10.1016/j.watres.2024.121946
42. Chen T. (2020). Basin boundary dataset of lakes over 10 km^2 in China. *Lake-Watershed Science Data Center, National Earth System Science Data Center, National Science & Technology Infrastructure of China.* DOI: 10.11971/lim.2023.003.db.pro2018YFD1100100
43. GEBCO Compilation Group (2023). GEBCO 2023 Grid. DOI:10.5285/f98b053b-0cbc-6c23-e053-6c86abc0af7b
44. McGarigal K., Cushman S. A., Neel M. C., et al. (2002). FRAGSTATS: Spatial pattern analysis program for categorical maps (Version 4.2). Available at: https://www.fragstats.org/index.php
45. Fang C., Song C., Wang X., et al. (2024). A novel total phosphorus concentration retrieval method based on two-line classification in lakes and reservoirs across China. *Sci. Total Environ.* 906:167522. DOI:10.1016/j.scitotenv.2023.167522
46. Li S., Song K., Wang S., et al. (2021). Quantification of chlorophyll-a in typical lakes across China using Sentinel-2 MSI imagery with machine learning algorithm. *Sci. Total Environ.* 778:146271. DOI:10.1016/j.scitotenv.2021.146271
47. Liu D., Duan H., Loiselle S., et al. (2020). Observations of water transparency in China's lakes from space. *Int. J. Appl. Earth Obs. Geoinf.* 92:102187. DOI:10.1016/j.jag.2020.102187
48. Qin B., Zhou J., Elser J. J., et al. (2020). Water depth underpins the relative roles and fates of nitrogen and phosphorus in lakes. *Environ. Sci. Technol.* 54:3191–3198. DOI:10.1021/acs.est.9b05858
49. Miller A., Panneerselvam J. and Liu L. (2022). A review of regression and classification techniques for analysis of common and rare variants and gene-environmental factors. *Neurocomputing* 489:466–485. DOI:10.1016/j.neucom.2021.08.150
50. Breiman L., Cutler A., Liaw A., et al. (2024). randomForest: Breiman and Cutlers Random Forests for Classification and Regression. CRAN: R-Project. https://cran.r-project.org/web/packages/randomForest/
51. Kuhn M., Wing J., Weston S., et al. (2024). caret: Classification and Regression Training. CRAN: R-Project. https://cran.r-project.org/web/packages/caret/index.html
52. Liaw A., & Wiener M. (2002). Classification and regression by randomForest. *R News* 2:18–22.https://journal.r-project.org/articles/RN-2002-022
53. Karsoliya S. (2012). Approximating number of hidden layer neurons in multiple hidden layer BPNN architecture. *Int. J. Eng. Trends Technol.* 3:714–717. DOI:10.14445/22315381/IJETT-V3I6P206
54. Biecek P., Maksymiuk S. and Baniecki H. (2025). DALEX: moDel Agnostic Language for Exploration and eXplanation. *CRAN: R-Project.* https://cran.r-project.org/web/packages/DALEX/index.html
55. Greenwell B. (2024). fastshap: Fast Approximate Shapley Values. CRAN: R-Project. https://cran.r-project.org/web/packages/fastshap/index.html
56. Lundberg S. M., Erion G., Chen H., et al. (2020). From local explanations to global understanding with explainable AI for trees. *Nat. Mach. Intell.* 2:56–67. DOI:10.1038/s42256-019-0138-9
57. Gong P. (2018). Global land use/land cover prediction dataset FROM-GLC-simulation. *National Earth System Science Center.* http://www.geodata.cn
58. Hurtt G. C., Chini L. P., Frolking S., et al. (2011). Harmonization of land-use scenarios for the period 1500–2100: 600 years of global gridded annual land-use transitions, wood harvest, and resulting secondary lands. *Clim. Change* 109:117–161. DOI:10.1007/s10584-011-0153-2
59. Xu Y., Xu X. and Tang Q. (2016). Human activity intensity of land surface: Concept, methods and application in China. *J. Geogr. Sci.* 26:1349–1361. DOI:10.1007/s11442-016-1331-y
60. Tang Q., Hua L., Cao Y., et al. (2024). Human activities are the key driver of water erosion changes in northeastern China. *Land Degrad. Dev.* 35:62–75. DOI:10.1002/ldr.4897
61. Alewell C., Ringeval B., Ballabio C., et al. (2020). Global phosphorus shortage will be aggravated by soil erosion. *Nat. Commun.* 11:4546. DOI:10.1038/s41467-020-18326-7
62. Liu X., Liu H., Xig J., et al. (2023). How the land use/cover changes and environmental factors at different scales affect lake water quality in arid and semi-arid regions. *Front. Ecol. Evol.* 11:1188927. DOI:10.3389/fevo.2023.1188927
63. Yi Y., Zhong J., Bao H., et al. (2021). The impacts of reservoirs on the sources and transport of riverine organic carbon in the karst area: A multi-tracer study. *Water Res.* 194:116933. DOI:10.1016/j.watres.2021.116933
64. Chen X. F., Chuai X. M. and Yang L. Y. (2014). Status quo, historical evolution and causes of eutrophication in lakes in typical lake regions of China. *Journal of Ecology and Rural Environment* 30:438–443. https://ere.ac.cn/en/article/id/10723
65. Guan Q., Feng L., Hou X., et al. (2020). Eutrophication changes in fifty large lakes on the Yangtze Plain of China derived from MERIS and OLCI observations. *Remote Sens. Environ.* 246:111890. DOI:10.1016/j.rse.2020.111890
66. Miller J. D. and Hutchins M. (2017). The impacts of urbanisation and climate change on urban flooding and urban water quality: A review of the evidence concerning the United Kingdom. *J. Hydrol. Reg. Stud.* 12:345–362. DOI:10.1016/j.ejrh.2017.06.006
67. Ji P., Chen J., Chen R., et al. (2024). Nitrogen and phosphorus trends in lake sediments of China may diverge. *Nat. Commun.* 15:2644. DOI:10.1038/s41467-024-46968-4
68. Chang D. (1981). The vegetation zonation of the Tibetan Plateau. *Mountain research and development* 1:29-48. DOI:10.2307/3672945
69. Lee M., Stock C. A., Shevliakova E., et al. (2024). Uneven consequences of global climate mitigation pathways on regional water quality in the 21st century. *Nat. Commun.* 15:5464. DOI:10.1038/s41467-024-49866-x
70. Wetland International (2016). Wetlands and biofuels. Available at: https://www.wetlands.org/case-study/wetlands-and-biofuels/ (Accessed: 17 March 2025)
71. Wang M., Janssen A. B., Bazin J., et al. (2022). Accounting for interactions between Sustainable Development Goals is essential for water pollution control in China. *Nat. Commun.* 13:730. DOI:10.1038/s41467-022-28351-3
72. Thomson A. M., Calvin K. V., Smith S. J., et al. (2011). RCP4.5: A pathway for stabilization of radiative forcing by 2100. *Clim. Change* 109: 77-94. DOI:10.1007/s10584-011-0151-4
73. Tian D., Guo Y. and Dong W. (2015). Future changes and uncertainties in temperature and precipitation over China based on CMIP5 models. *Adv. Atmos. Sci.* 32:487–496. DOI:10.1007/s00376-014-4102-7
74. Cheng Y., Liu H., Du J., et al. (2025). Quantifying biodiversity's present and future: Current potentials and SSP - RCP - driven land use impacts. *Earth's Future* 13:e2024EF005191. DOI:10.1029/2024EF005191
75. Xu F., Zhang G., Woolway R. I., et al. (2024). Widespread societal and ecological impacts from projected Tibetan Plateau lake expansion. *Nat. Geosci.* 17:516–523. DOI:10.1038/s41561-024-01446-w
76. Zhang Q., Yang J., Wang W., et al. (2021). Climatic warming and humidification in the arid region of Northwest China: Multi-scale characteristics and impacts on ecological vegetation. *J. Meteorolog. Res.* 35:113–127. DOI:10.1007/s13351-021-0105-3
77. Wei F., Cui S., Liu N., et al. (2021). Ecological civilization: China's effort to build a shared future for all life on earth. *Natl. Sci. Rev.* 8:nwaa279. DOI:10.1093/nsr/nwaa279

FUNDING AND ACKNOWLEDGMENTS

This work was supported by the National Natural Science Foundation of China (U23A2008), the funding from Youth Innovation Promotion Association of CAS (2017277), and the Young Scientist Group Project of Northeast Institute of Geography and Agroecology, Chinese Academy of Sciences (2022QNXZ03). The funders had no role in study design, data collection and analysis, decision to publish, or preparation of the manuscript.

AUTHOR CONTRIBUTIONS

Xinying Shi: Methodology, Formal Analysis, Investigation, Visualization, Original Draft Preparation. Dehua Mao: Conceptualization, Validation, Funding acquisition, Project Administration, Writing – review & editing. Ling Luo: Writing – review & editing. Kaishan Song: Writing – review & editing. Hongtao Duan: Writing – review & editing. Sijia Li: Data Curation, Validation, Writing – review & editing, Chong Fang: Data Curation, Validation, Writing – review & editing. Dong Liu: Data Curation, Validation, Writing – review & editing. Hui Tao: Data Curation. Hengxing Xiang: Writing – review & editing. Zongming Wang: Supervision. All authors contributed to the manuscript and approved the final version.

DECLARATION OF INTERESTS

The authors declare no competing interests.

DATA AND CODE AVAILABILITY

The per-lake datasets used in this study — including LPMs (with lake coordinates), and annual TLI, Chl-a, TP, and SDD values—have been deposited in DOI:10.5281/zenodo.15751520. Lake identifiers in each table correspond exactly to the OBJECTID field in the China Lake Dataset,[40] allowing users to cross-reference and retrieve additional information.

LEAD CONTACT WEBSITE

Dehua Mao: https://neigae.cas.cn/sourcedb/zw/expert/201612/t20161213_6198559.html